Materials Science Forum
ISSN: 1662-9752, Vol. 1183, pp 69-79
doi:10.4028/p-I1nbWq

Submitted: 2026-01-19
Revised: 2026-02-14
Accepted: 2026-02-24
Online: 2026-04-13

A Qualitative Study of the Contact Pressure Distribution in Cold Rolling

Shaheryar Younas[1,a*], Jos Havinga[1,b], Camile Hol[2,c], Ton van den Boogaard[1,d]

[1]Faculty of Engineering Technology, University of Twente, Netherlands

[2]Tata Steel Nederland B.V.

[a]s.younas@utwente.nl, [b]jos.havinga@utwente.nl, [c]camile.hol@tatasteeleurope.com, [d]a.h.vandenboogaard@utwente.nl

Keywords: Cold Rolling, Roll Force, Friction Hill, Anisotropy, Plane Strain Point

Abstract Cold rolling forces are strongly affected by lubrication and material properties, and may potentially be used to estimate material property variations along the coil. The 1D slab method is commonly used to estimate rolling forces as it is computationally inexpensive. By model definition, the pressure distribution as modelled in the slab method has a single peak or friction hill in the roll bite. However, it has been observed in several studies that multiple local peaks can appear in the pressure distribution in the roll bite. Additionally, material anisotropy also affects the contact pressure distribution and steady state roll force. In the present work, a 2D plane strain finite element rolling model is used for a detailed sensitivity study of the multitude of parameters that affect the vertical pressure distribution and the steady state roll force. The considered model parameters are material anisotropy, entry sheet thickness, roll radius, tensions, coefficient of friction and roll gap.

Introduction

Prediction of rolling force has been a topic of research for decades, with models ranging from analytical relations and one-dimensional slab models up to detailed finite element (FE) simulations. Roll force predictions are relevant for controlling the roll gap and ensuring robust production conditions. In addition to that, roll forces and torques are affected by material property variations, and may therefore potentially be used to assess the evolution of material properties over rolling stands [1,2]. For this specific purpose, a precise description of the effect of process conditions and incoming material properties on the rolling force is required.

Friction plays a key role in the sheet rolling process. At the entry zone, the sheet speed is lower than the roll speed, meaning that the relative velocity of the sheet with respect to the roll is backward. The friction force will therefore act in the forward direction and help pull the sheet into the roll bite. In the exit zone, the relative velocity of the sheet with respect to the roll is forward, meaning that the frictional force acts in the backward direction. In between the forward and backward slipping regions, there is a stick zone, where the roll and sheet speeds are equal [3]. In several two-dimensional models, the stick region is represented as a point along the contact arc between the roll and the sheet, which is called the neutral point. When the process conditions are such that the forward and backward slipping region are established, with a neutral zone in between, steady state rolling is achieved. Otherwise, certain combinations of process conditions and material properties may result in only forward or backward slip, meaning that the process conditions are unstable.

Several modeling approaches have been developed to predict sheet rolling forces and deformations. A popular cold rolling model in industry is the slab model due to its computational speed. It divides the sheet into one-dimensional elements called slabs, applies force equilibrium to get the differential equation describing pressure distribution and then integrates over sheet length. It was first developed by Von Karman in 1925 who also gave the concept of neutral point. Later, Orowan improved the model by including strain hardening and roll elastic deformation [4]. An important result from Orowan's model is the vertical pressure distribution along the roll bite, also called as friction hill which helps in understanding the process. The roll contact pressure increases from the entry side, reaches maximum pressure and then decreases towards the exit zone. The point of maximum pressure

represents the neutral point along the sheet length. Another important parameter is the reaction force applied by the roll on the sheet upon contact, which is also called the roll force. As the roll force is commonly measured in industrial rolling processes, it is often used as an indicator of changes in process conditions.

Several extensions of the slab method have been developed to improve prediction accuracy and the applicability of the model, for example for asymmetric rolling, while benefiting of its low computational cost [5]. On the other side, several researchers have used the FE method to obtain a more accurate description of the sheet and roll deformations in the roll bite, at the expense of increased computational cost. While Orowan's model is a one-dimensional representation of the problem that accounts for a single peak of the vertical pressure distribution, several studies have reported multiple pressure peaks when FE models are used [5,6]. These pressure peaks appear as oscillations on top of a pressure distribution that is similar to the one obtained with the slab method. Recently, a semi-analytic model that uses multiple-scales asymptotics has been developed, that is able to describe stress and strain oscillations in rolling direction and through thickness under the assumption of rigid plastic material deformation. This model can be used to describe pressure oscillations with a computational cost in the order or seconds [7].

Besides the need to describe pressure oscillations for obtaining a more accurate rolling force prediction, another factor that is commonly not accounted for in two-dimensional rolling models is the effect of material anisotropy [8]. Cold rolling generates anisotropy in the sheet due to texture evolution. As plane strain conditions apply in most of the sheet (expect at the edges) during rolling, it is important to use anisotropic material models to account for the position of the plane strain point in the yield locus correctly, even while modeling the process in 2D.

This study aims to determine qualitative effect of various cold rolling input parameters such as plane strain point, sheet thickness, roll radius, coefficient of friction, tensions and unloaded roll gap fraction on vertical pressure distribution, friction hills and steady state roll force through sensitivity analysis using a FE model of the process. Analysis has been done using both isotropic and anisotropic hardening. The contents of the paper are divided in the following way: in section "Cold Rolling Model", details of the cold rolling model are given. In section "Sensitivity Analysis", strategy of sensitivity analysis of input parameters of cold rolling model is discussed, followed by the sections "Results and Discussion" and "Conclusion".

Cold Rolling Model

Specifications. This section describes specifications of the cold rolling model developed using commercial Finite Element (FE) software ABAQUS which is used for the sensitivity analysis. In this work, the following coordinate directions are used for stress and strain: the 11-direction represents the sheet length direction, the 22-direction represents the sheet width direction and the 33-direction represents the sheet thickness direction.

When the sheet width is significantly larger than the thickness, cold rolling can be considered as a plane strain process, meaning that the strain in width direction is zero ($\varepsilon_{22} = 0$). Therefore, the process can be modeled in 2D. An implicit dynamic simulation is used to roll a sheet section until steady state conditions are reached. To reduce the computational time, a single work roll and half the sheet thickness is modeled by assuming symmetry about the 11-axis. A partial deformable roll is modeled, with high mesh density around the contact zone.

The roll angular velocity has a constant value of almost 42 rad$\cdot$s^{-1}. The sheet position is initialized just in front of the roll bite, with zero initial velocity, and prescribed front and back tensions T_{in} and T_{out}. The displacement of the sheet is force controlled: the difference between prescribed front and back tension ΔT will pull the sheet into the roll bite, and will continue to accelerate the sheet until the sheet tensions equilibrate with the roll contact forces and steady state is reached. A mild steel material model is used with tabulated hardening and a Hill yield locus. The nominal hardening curve yields

at 304 MPa and saturates at 0.6 equivalent plastic strain at a value of 566 MPa. A constant Coulomb friction parameter is used for the contact between the roll and the sheet. The values of the different model parameters will be presented in the section “Sensitivity Analysis”.

The work roll is meshed with gradually increasing mesh density from its inner region to the outer region that is in contact with the sheet. The total number of elements and nodes in the work roll are 54.448 and 46.051 respectively. The total number of elements and nodes in the sheet are 12.810 and 13.740 respectively, with 15 elements through thickness of the sheet. With this mesh, approximately 105 sheet elements are in contact with the roll in the contact zone in the base simulation. As the model is 2D, the computational time for implicit dynamic analysis still remains reasonable.

Implementation of Anisotropic Effect in the Model. Material anisotropy has a significant effect on the roll force, and must therefore be accounted for in the model [8]. Specifically, it is important to consider that material anisotropy evolves over rolling stands. In this study, the Hill 48 yield criterion is used. It is considered that it is not beneficial to use a more advanced yield criterion, as the plane strain point of the yield locus is the only relevant part of the yield locus when modeling 2D plane strain rolling. The Hill yield locus is a quadratic yield criterion resulting in an ellipsoidal shape in 3D:

$$F(\sigma_{11}-\sigma_{22})^2 + G(\sigma_{22}-\sigma_{33})^2 + H(\sigma_{33}-\sigma_{11})^2 + 2L\sigma_{23}^2 + 2M\sigma_{31}^2 + 2N\sigma_{12}^2 = \sigma_{eq}^2 \tag{1}$$

Where σ_{11}, σ_{22}, σ_{33} are normal stresses, σ_{12}, σ_{23} and σ_{31} are shear stresses and F, G, H, L, M and N are Hill parameters.

In the above-mentioned study where the effect of anistotropy in cold rolling was characterized, planar anisotropy was assumed, and the Lankford parameter in rolling direction was used to parametrize the anisotropy, using a Hill yield locus. In that case, the plane strain stress in rolling direction $\sigma_{11,\mathrm{PS}}$ and in transverse direction $\sigma_{22,\mathrm{PS}}$ are directly defined by the Lankford parameter in rolling direction. Alternatively, in this work it is chosen to decouple the effect of both stress components in the plane strain point, to identify whether these components have an independent effect on the rolling conditions. To do so, the relation between the Hill yield locus parameters F, G and H, the plane strain stress components $\sigma_{11,\mathrm{PS}}$ and $\sigma_{22,\mathrm{PS}}$, and the yield stress σ_y has been determined, and used to find the values of the Hill parameters as function of the stress values at the plane strain point:

$$F = \frac{\left(\sigma_{11,\mathrm{PS}}^2 - \sigma_y^2\right)\left(\sigma_{11,\mathrm{PS}} - \sigma_{22,\mathrm{PS}}\right)}{\sigma_{11,\mathrm{PS}}\,\sigma_{22,\mathrm{PS}}^2} \tag{2}$$

$$G = 1 - \frac{\sigma_{11,\mathrm{PS}}^2 - \sigma_y^2}{\sigma_{11,\mathrm{PS}}\,\sigma_{22,\mathrm{PS}}} \tag{3}$$

$$H = \frac{\sigma_{11,\mathrm{PS}}^2 - \sigma_y^2}{\sigma_{11,\mathrm{PS}}\,\sigma_{22,\mathrm{PS}}} \tag{4}$$

In determining these relations, plane stress in thickness direction ($\sigma_{33,PS} = 0$) and plane strain in width direction ($\epsilon_{22} = 0$) were assumed, meaning that the used parametrization of the material properties respresent the plane strain point with in-plane loads only, despite the fact that the actual stress state in rolling is not a plane stress condition. The other parameters L, M and N were taken as constants, equal to 1.5, being the coefficients from the isotropic case.

Sensitivity Analysis

A detailed sentitivity study is performed, to characterize the effect of different parameters on the vertical pressure distribution in cold rolling. The set of performed simulations can be categorized in three different groups:

Group I: Sensitivity to stress components of plane strain point. This set of simulations is performed to study the effect of both stress components of the plane strain point on the rolling force. With the plane strain point of an isotropic yield locus being defined as a reference point with stress values $\bar{\sigma}_{11,\mathrm{PS}}$ and $\bar{\sigma}_{22,\mathrm{PS}}$, both stress components were varied with -5% and +5%. With minimum, nominal and maximum values for $\sigma_{11,\mathrm{PS}}$ and for $\sigma_{22,\mathrm{PS}}$, a total of 9 positions of the plane strain point have been analyzed, as visualized in Fig. 1.

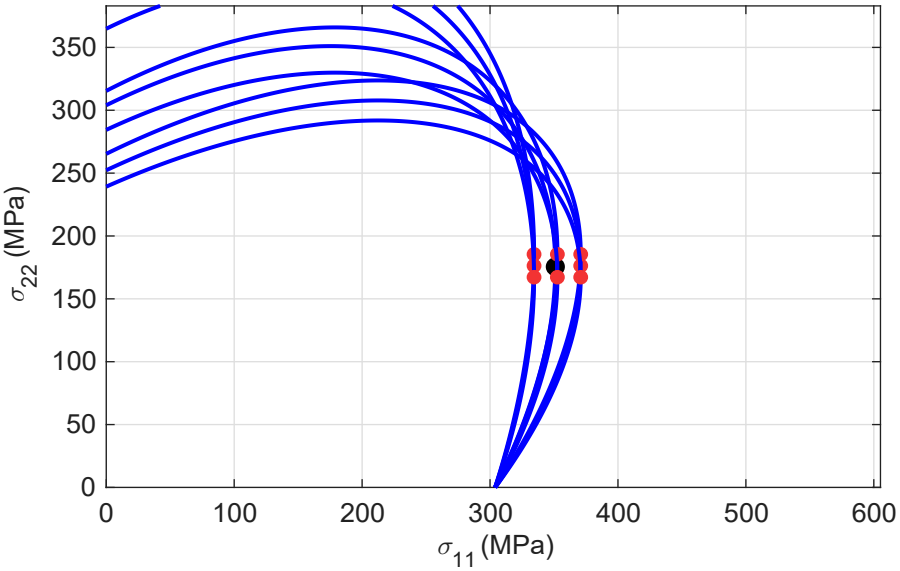

Fig. 1: Hill yield loci used in sensitivity study of stress components of plane strain point.

Besides the above-mentioned simulations, two sets of Hill yield locus parameters have been identified with exactly the same plane strain points, but with different uniaxial yield stress values, to verify that the results are completely dependent on the plane strain point values and independent of the uniaxial yield stress value.

Group II: Sensitivity to unloaded roll gap fraction. The unloaded roll gap fraction is defined as the unloaded roll gap distance divided by the undeformed sheet thickness. In case of rigid rolls and no elastic springback, the final thickness of the sheet will be equal to the unloaded roll gap. In the simulations, roll deformation and springback is accounted for, meaning that the final sheet thickness will be larger than the unloaded roll gap distance. Simulated roll gap fractions vary from 50% to 90% with steps of 10%.

These simulations are performed for a material model with isotropic properties, and for a material model with anisotropic properties. The plane strain point of the anisotropic model is defined as $\sigma_{11,\mathrm{PS}} = 1.22 \cdot \sigma_y$ and $\sigma_{22,\mathrm{PS}} = 0.58 \cdot \sigma_y$ (such that $\sigma_{22,\mathrm{PS}}/\sigma_{11,\mathrm{PS}} = 0.475$) where $\sigma_{11,\mathrm{PS}}$ and $\sigma_{22,\mathrm{PS}}$ are normal stresses in the length and width direction under plane strain condition. Note that the ratio $\sigma_{22,\mathrm{PS}}/\sigma_{11,\mathrm{PS}}$ equals 0.5 for isotropic materials.

Group III: Sensitivity to other process parameters. Finally, a set of simulations is performed to assess the sensitivity of the roll pressure distribution to different model parameters, by evaluating a one-at-a-time (OAT) design of experiments in which a set of base settings is defined, and one parameter at a time is varied to its minimum and maximum values. The set of analyzed parameters and used ranges are given in Table 1.

The front and back tensions are parametrized using the difference of tensions $\Delta T = T_{out} - T_{in}$ and the average tension $T_{avg} = (T_{out} + T_{in})/2$, as these parameters better characterize the set of realistic sheet tension values that are used in sheet rolling. ΔT determines the friction force in longitudinal direction that is required to reach steady state conditions. T_{avg} determines amount of stretch in the sheet.

Table 1: Base values and deviations of parameters used in the rolling model.

Parameter	Base values	Deviation from the base values
Sheet thickness h_i	1.825 mm	$\pm$10%
Roll radius R	240 mm	$\approx \pm$5%
Unloaded roll gap fraction (% of sheet thickness)	90%	50% to 90%
Coefficient of friction μ	0.07	$\pm$30%
Difference of front and back tensions ΔT	123.9 kN/m	$\pm$10%
Average tensions T_{avg}	280.8 kN/m	$\pm$10%

Results and Discussion

The results of the different analyses are presented below.

Group I: Sensitivity to stress components of plane strain point.

The roll pressure distributions for the simulations with varying plane strain points are presented in Fig.2. As expected, the plane strain stress component in length direction $\sigma_{11,\text{PS}}$ has a significant effect on the pressure distribution. On the other hand, it can be observed that the 22-direction stress component of the plane strain point has minimal effect on the pressure distribution. The roll forces are also shown in the contour plot of Fig. 3, showing that the effect of $\sigma_{11,\text{PS}}$ is significant while the effect of $\sigma_{22,\text{PS}}$ is negligible.

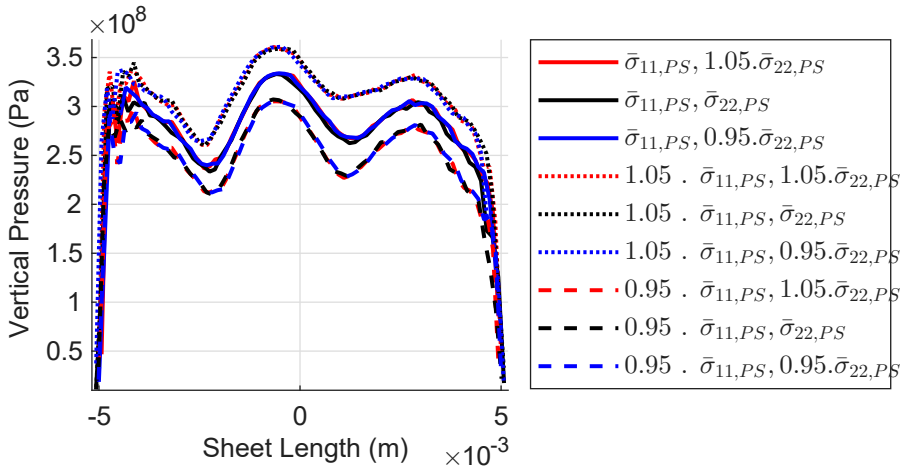

Fig. 2: Vertical Pressure Distribution

In this study, it is also verified that only the location of the plane strain point in stress space is relevant for rolling, whereas the actual value of uniaxial yield stress σ_y does not directly affect the roll force. This was done by defining two material models with equal plane strain point location but distinct yield stress values. The corresponding stress values are given below, and the yield loci are shown in Fig. 4.

Case 1: $\sigma_y = 304$ MPa, $\sigma_{11,\text{PS}} = 370.88$ MPa, $\sigma_{22,\text{PS}} = 176.32$ MPa.

Case 2: $\sigma_y = 334.4$ MPa, $\sigma_{11,\text{PS}} = 370.88$ MPa, $\sigma_{22,\text{PS}} = 176.32$ MPa.

The only difference between the results that could have been expected is the part of the deformation path when a material point moves from elastic to plastically deforming, as the stress state under elastic

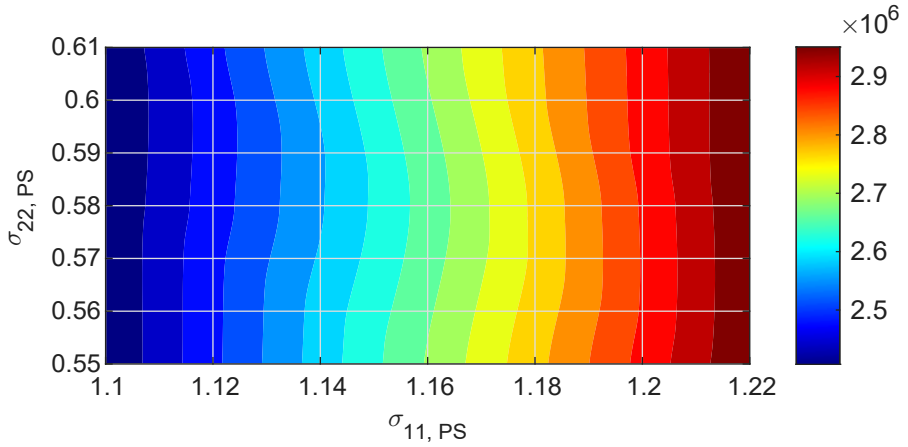

Fig. 3: Contour plot of steady state rolling force w.r.t. σ_{11} and σ_{22}.

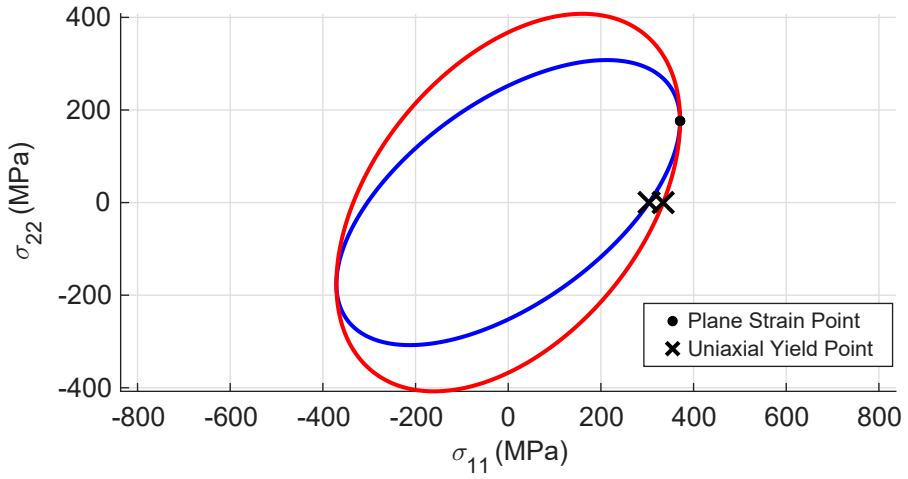

Fig. 4: Hill yield loci for cases 1 and 2.

deformation with a Poisson ratio ν of 0.3 does not reach the yield locus at its plane strain point. However, this effect is minimal, and it was observed that the roll force and roll pressure distribution for both cases is identical, with a steady state roll force value of approximately 2600 kN/m.

Group II: Sensitivity to unloaded roll gap fraction.

The steady state roll force computed with the isotropic and anisotropic models is shown in Fig. 5. It increases with unloaded roll gap fraction as the thickness reduction and the length of the arc of contact increase. Note that the force is slightly higher for the anisotropic case, as the 11-direction stress component of the plane strain point is higher than in the isotropic case, being $\sigma_{11,\mathrm{PS}} = 1.22 \cdot \sigma_y$.

When examining the vertical stress distribution in the roll gap for the isotropic and anisotropic cases in Fig. 6, it can be seen that the contact length increases and that the pressure also increases, leading to a higher roll force. The oscillations in the vertical pressure are apparent, and correspond with the observations in other studies [5,6,7]. The number of oscillations increases with decreasing roll gap, as listed in Table 2. It can also be observed that the amplitude of the oscillations decreases with increasing number of oscillations. Note that it is essential to have a large number of sheet and roll elements in the contact zone to identify these detailed oscillations in the pressure distribution.

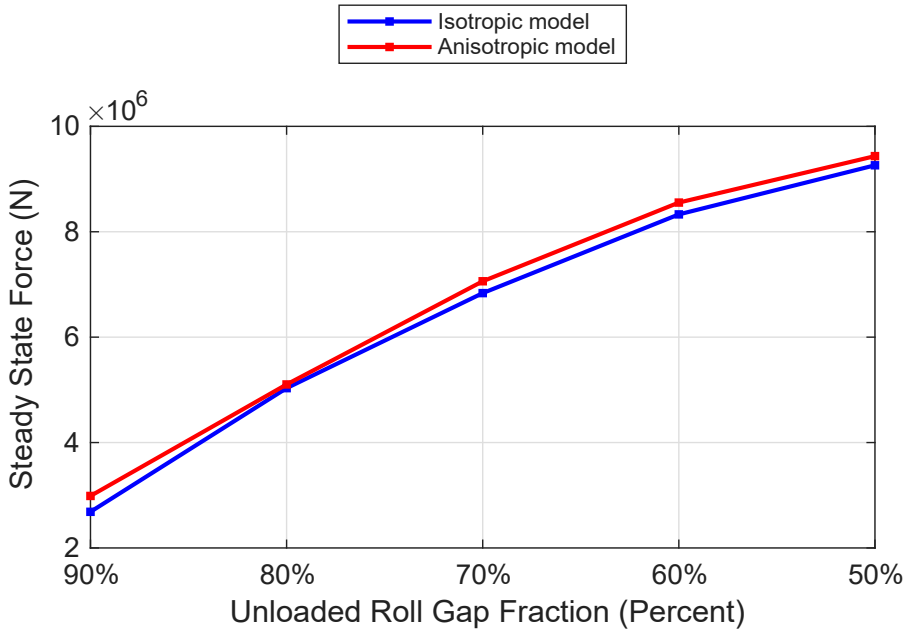

Fig. 5: Roll force Line Plots for Different Unloaded Roll Gap Fractions (Percent)

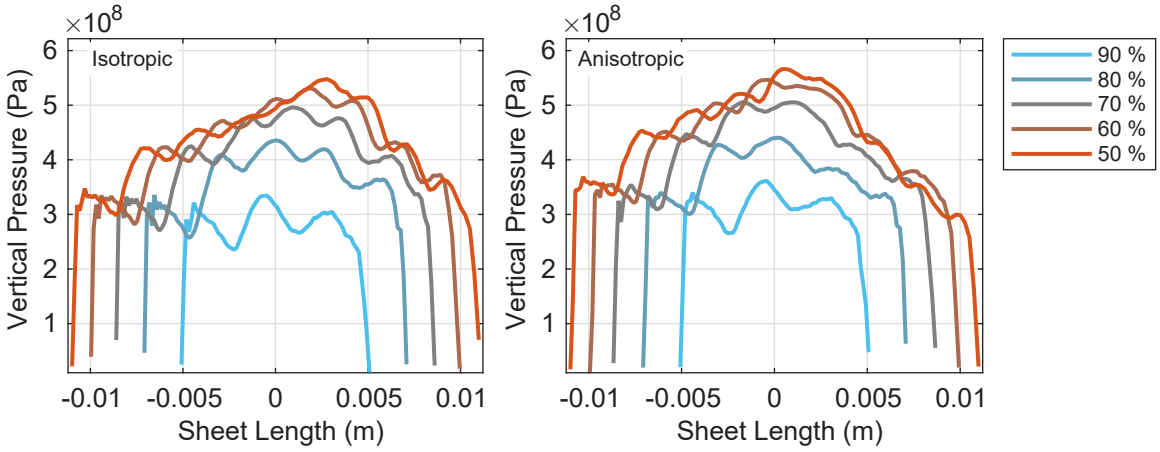

Fig. 6: Vertical Roll Pressure Distribution for Varying Unloaded Roll Gap Fractions (Percent)

Table 2: Number of oscillations in the vertical pressure for different unloaded roll gap fractions.

Unloaded roll gap fraction		90%	80%	70%	60%	50%
Number of oscillations	**Isotropic Model**	3	5	6	8	7
	Anisotropic Model	3	5	6	7	9

Group III: Sensitivity to other process parameters.

The effects of sheet thickness, roll radius and friction coefficient on the total roll force are presented in Fig. 7. It is observed as expected that the roll force increases with increasing sheet thickness, roll radius and friction coefficient.

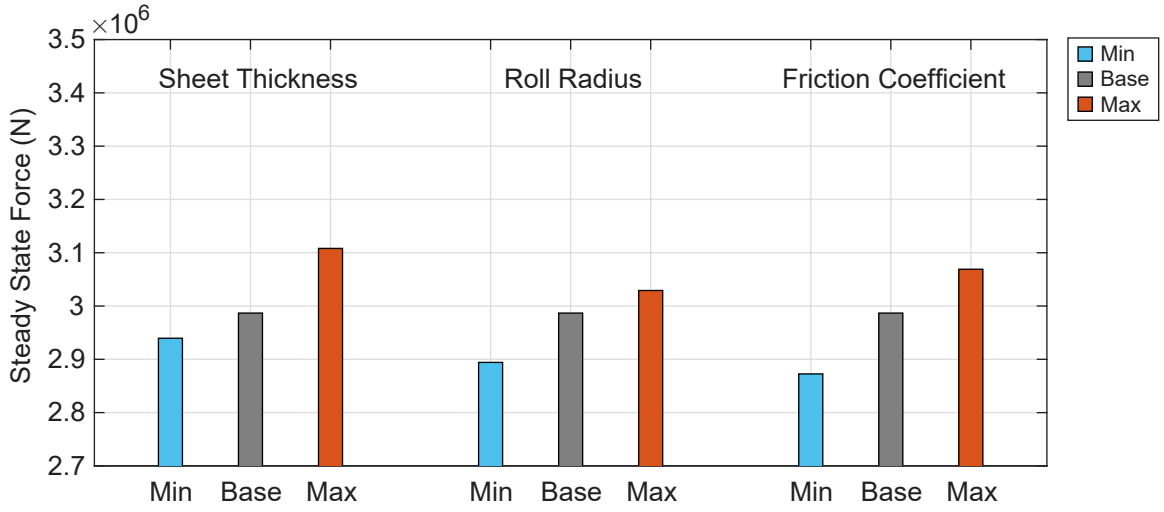

Fig. 7: Roll force values for different sheet thicknesses, roll radii and coefficients of friction.

Sheet thickness.

The increase of steady state roll force with increasing sheet thickness can be understood from the following cold rolling relations [9,10]:

$$L \approx \sqrt{R\Delta h} = \sqrt{R(h_o - h_i)} = \sqrt{Rh_i\left(\frac{h_o}{h_i} - 1\right)} = \sqrt{Rh_i\left(\frac{1}{r} - 1\right)}$$

$$\Rightarrow L \propto \sqrt{h_i} \tag{5}$$

$$F_r = bL\sigma_f\left(1 + \frac{\mu L}{h_m}\right) \tag{6}$$

Where L is the length of the arc of contact, R is the roll radius, h_i is the input sheet thickness, h_o is the output sheet thickness, r is the thickness reduction, F is the roll force, b is the sheet width, σ_f is the flow stress, μ is the friction coefficient and $h_m = (h_o + h_i)/2$ is the average thickness. Equation (5) shows that when the sheet thickness increases, the length of the arc of contact between sheet and the roll also increases. As a result, roll force also increases according to Equation (6), which is known as Sims formula.

The effect of thickness variation on the vertical pressure distribution is shown in Fig.8a. The location of the oscillations shifts with varying thickness, which can be understood from the observation that the ratio between sheet thickness and contact zone length determine the number of oscillations in the pressure distribution [7]. It can even be observed in Fig. 8a that the number of peaks in the pressure distribution is four for the lowest thickness, and three for the other two cases. This also explains why the increase of the roll force in the sensitivity study is not linear, as can be seen in Fig. 7.

The steady state force increases with increasing roll radius, as shown in Fig. 7. The reason is that a larger roll radius increases the length of the arc of contact, and thereby also increases the roll force. However, the effect of roll radius on the pressure distributions is not very significant, as seen in Fig. 8b. The width of the pressure distribution is slightly affected by the roll radius, but the pressure distribution within the contact zone is close to equal in all cases.

Coefficient of friction.

Like sheet thickness and roll radius, it can be seen in Fig. 7 that steady state force also increases with increasing coefficient of friction. The explanation is that the pressure gradient increases with

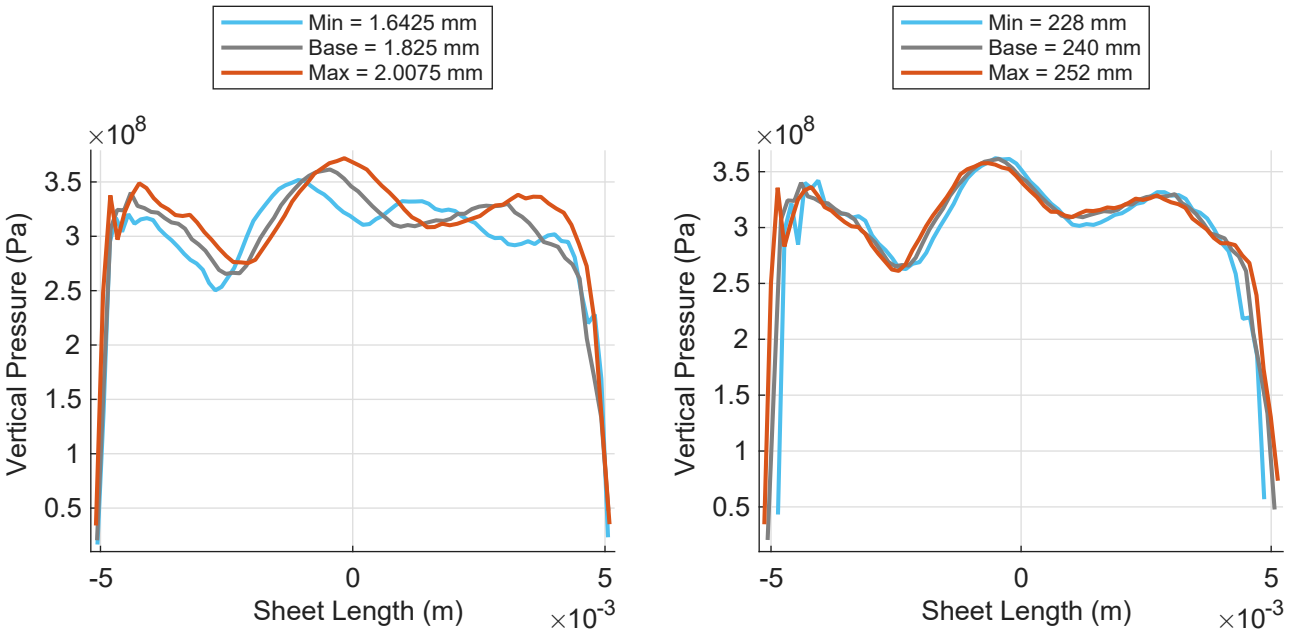

(a) Effect of sheet thickness

(b) Effect of roll radius

Fig. 8: Vertical pressure distribution due to variation in roll radius and sheet thickness.

coefficient of friction according to the Orowan's model:

$$\frac{dp}{dx} = -\frac{+2\mu p}{h} + 2\frac{dk}{dx} \tag{7}$$

Where p is the vertical pressure, x is the distance along the sheet length, μ is the coefficient of friction, h is the exit thickness and k is the shear strength. As per Equation (7), the pressure increases with increasing friction coefficient, as can be seen in Fig. 9. With varying friction small changes in the position of the oscillations in the pressure distribution can be observed..

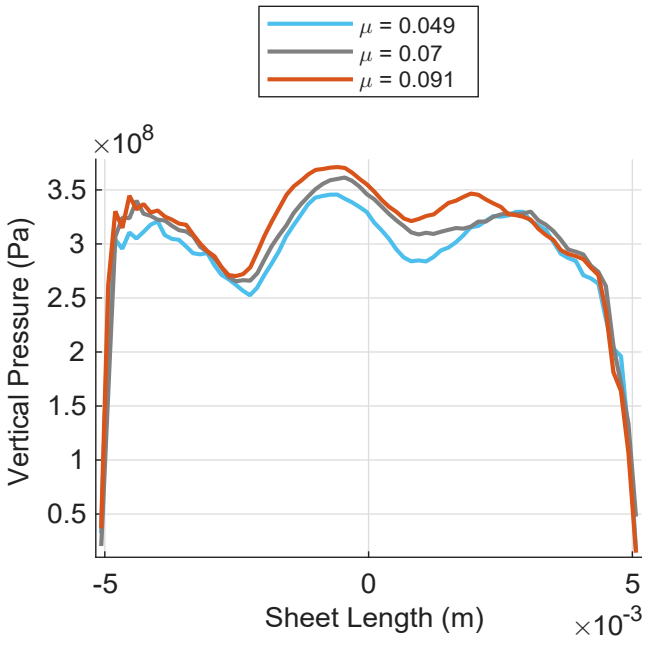

Fig. 9: Vertical pressure distribution for different friction coefficients.

Front and Back Tensions.

As mentioned in Section "Sensitivity analysis", front and back tensions have been analyzed by varying the tension difference ΔT and the average tension T_{avg}. Note that the steady state roll force increases with increase in both ΔT and T_{avg}. The reason behind influence of ΔT is that it governs the net force which pulls the sheet through the roll bite. Therefore, the roll has to work lesser if ΔT and the net force is higher. The reason behind influence of T_{avg} is that it governs the stretch in the sheet along longitudinal direction due to the tensions applied in the opposite directions. This makes rolling relatively easier and we see decrease in rolling force. the effect of T_{avg} is more significant. Further, it can be seen that the steady state roll force remains the highest for the base cases. Vertical pressure distribution also follows a similar pattern (fig. 11) where the upward shift of pressure is more noticeable for variation in T_{avg}.

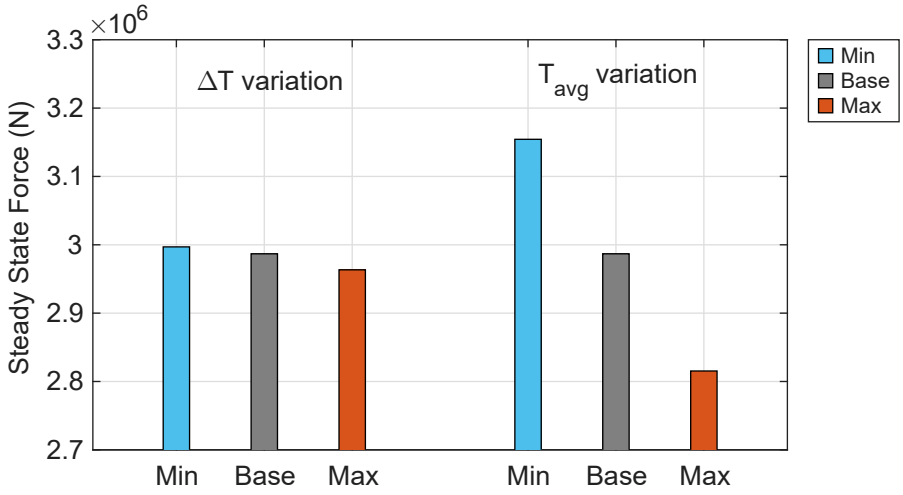

Fig. 10: Roll force values for different values of tension difference ΔT and of average tension T_{avg}.

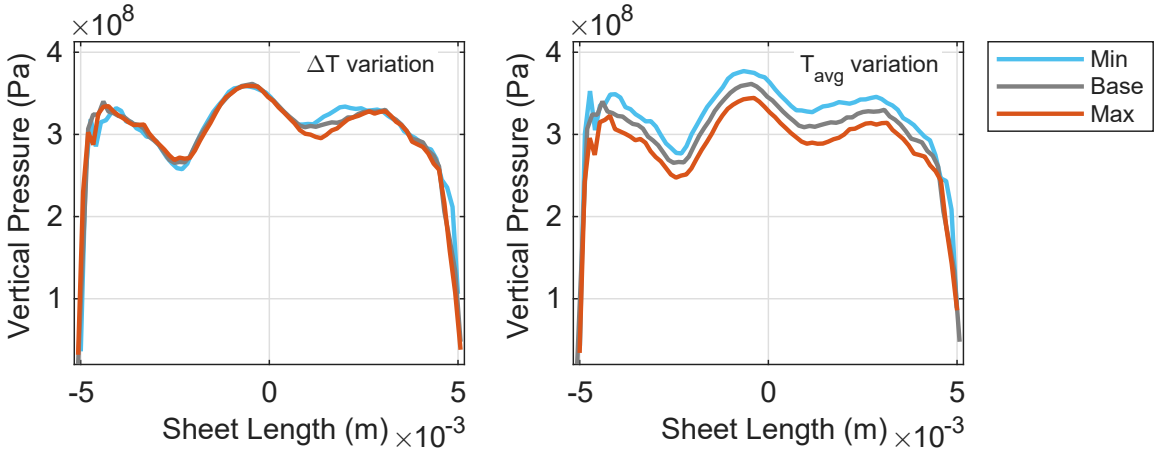

Fig. 11: Vertical pressure distributions for for different values of tension difference ΔT and of average tension T_{avg}.

Conclusions

In this research, the effect of different cold rolling parameters on steady state roll force and vertical pressure distribution for isotropic and anisotropic models were studied qualitatively through sensitivity analysis. Based on the results, the following conclusions can be made:

1 The roll force is sensitive towards the longitudinal stress component of the plane strain point $\sigma_{11,\mathrm{PS}}$, and not sensitive to the transverse stress component of the plane strain point $\sigma_{22,\mathrm{PS}}$.

2 There can be several combinations of uniaxial yield point and plane strain point for which the roll force will be the same.

3 As known from literature, it is verfied that steady state roll force increases with increasing sheet thickness, roll radius and roll gap closure.

4 It has been observed that the steady state roll force increases with increase in ΔT and T_{avg}. However, the effect of T_{avg} is more prominent.

5 By modelling the contact zone in the FE model with a large number of elements on the roll and on the sheet, oscillations in the vertical pressure distribution in the roll gap could be observed in all simulations. The number of oscillations is strongly affected by the unloaded roll gap fraction, weakly affected by the sheet thickness, and not significantly affected by the other parameters that were varied in this study. Also, the amplitude of the oscillations decrease with the increasing number of oscillations in the roll gap.

Acknowledgements

This research was carried out under project number N21022d in the framework of the Partnership Program of the Materials innovation institute M2i (www.m2i.nl) and the Netherlands Organization for Scientific Research (www.nwo.nl).

References

[1] A. Del Prete and T. Primo: Inverse flow stress model validation in hot rolling with different thermal conditions, Int. J. Adv. Manuf. Technol. (2025), pp. 1–17

[2] D. Szeliga, M. Graf, R. Kawalla and M. Pietrzyk: Identification of material properties based on rolling process at 4-stand laboratory mill, AIP Conf. Proc. Vol. 1353 (2011), pp. 391–397

[3] Y. Shigaki, R. Nakhoul and P. Montmitonnet: Numerical treatments of slipping/no-slip zones in cold rolling of thin sheets with heavy roll deformation, Lubricants 3(2) (2015), pp. 113–131

[4] E. Orowan: The calculation of roll pressure in hot and cold flat rolling, Proc. Inst. Mech. Eng. 150(1) (1943), pp. 140–167

[5] P. Montmitonnet: Hot and cold strip rolling processes, Comput. Methods Appl. Mech. Eng. 195(48–49) (2006), pp. 6604–6625

[6] A.C.M. Miranda, C.L. Neto, W. da S. Labiapari, P.H.R. Pereira, P.R. Cetlin and A.R. Arias: Study of the coefficient of friction and forward slip in cold rolling of stainless steel AISI 430 in sendzimir mills, J. Mater. Res. Technol. 34 (2025), pp. 4912–923

[7] M. Erfanian, E.J. Brambley, F. Flanagan, D. O'Kiely and A.N. O'Connor: Through-thickness modelling of metal rolling using multiple-scales asymptotics, Eur. J. Mech. A/Solids (2025), p. 105712

[8] L.J.M. Jacobs, E.H. Atzema, J. Moerman and M.B. de Rooij: Quantification of the influence of anisotropic plastic yielding on cold rolling force, J. Mater. Process. Technol. 319 (2023), p. 118055

[9] R.B. Sims: The calculation of roll force and torque in hot rolling mills, Proc. Inst. Mech. Eng. 168(1) (1954), pp. 191–200

[10] W.L. Roberts: Cold rolling of steel, Routledge (2017)